JOURNAL OF Materials CHEMISTRY

Ordering and optical properties of monolayers and multilayers of silica spheres deposited by the Langmuir–Blodgett method†

Márta Szekeres,[a,b] Olexiy Kamalin,[a] Robert A. Schoonheydt,*[a] Kurt Wostyn,[c] Koen Clays,[c] André Persoons[c] and Imre Dékány[b]

[a]*Centrum voor Oppervlaktechemie en Katalyse, Katholieke Universiteit Leuven, Kasteelpark Arenberg 23, 3001 Leuven, Belgium. E-mail: Robert.Schoonheydt@agr.kuleuven.ac.be*
[b]*Department of Colloid Chemistry, University of Szeged, Aradi vt. 1, 6720 Szeged, Hungary*
[c]*Afdeling Chemische en Biologische Dynamica, Katholieke Universiteit Leuven, Celestijnenlaan 200D, 3001 Leuven, Belgium*

Received 15th May 2002, Accepted 2nd July 2002
First published as an Advance Article on the web 3rd October 2002

Monodisperse spherical silica particles (357, 450 and 550 nm in diameter) prepared by the method of Stöber were used to construct two-dimensional and three-dimensional structures with photonic bandgaps with the Langmuir–Blodgett technique. Floating monolayers of silica particles on water were made by using ionic surfactants, hexadecyltrimethylammonium bromide, decyltrimethylamonium bromide, sodium dodecylsulfate and octylbenzenesulfonic acid sodium salt. These monolayers were transferred onto glass microscope slides *via* vertical deposition. The effect of the type, concentration, and chain length of the surfactant, and the composition of the dispersion medium (chloroform, methanol, or a mixture of both) on the quality of particle ordering was investigated. The solvent was the most important parameter and the largest hcp crystalline areas were obtained with methanol. Up to 6 layers could be deposited. The photonic bandgaps for both monolayers and multilayers are observed at the wavelength predicted by theory. The height of the gap increases and the width decreases gradually as the number of layers increases. The incidence angle dependence of the transmission minimum of these structures also coincides with that predicted by theory: the position of the bandgap shifts with the angle of incidence [from 90 to 40° with respect to the (111) crystal plane] according to Bragg's law.

Introduction

Colloidal monosized particles have the ability to self assemble. The most well-known natural examples of such structures are gemstone opals. In opal minerals, amorphous SiO_2 spheres of uniform shape and size are crystallized into three-dimensional face-centered cubic structures, giving rise to iridescent colours.[1,2] It is of fundamental scientific interest to synthesize monodisperse colloidal particles and ordered colloidal superstructures. Crystallites of monodisperse colloidal particles—colloidal crystals—and the process of their formation deserve much attention from both theoretical and practical points of view. Since perfectly spherical and monodisperse colloidal particles can be prepared (mainly polymer latex and amorphous silica particles), it is possible to mimic the naturally occurring colloidal crystallization processes in the laboratory.

Colloidal stability, self assembly and aggregation of monodisperse spherical particles in suspension and at the interface between two fluid phases have been intensively studied to explore colloidal interactions and to establish the necessary conditions for crystal formation under laboratory conditions. Long-range attraction interactions were found to act during colloidal crystallization processes in concentrated suspensions.[3] The crystallization of charge-stabilized colloidal particles in two dimensions is directed by the repulsive dipole–dipole interactions between the particles acting through the air or oil phase.[4,5]

The practical interest of ordered colloidal assemblies stems from areas such as catalysis,[6] membranes,[7] sensors,[8–10] optoelectronics, and photonics.[11,12] For photonics one-, two- and three-dimensional photonic crystals have to be prepared with incomplete or complete photonic bandgaps in designed ranges of frequencies. The bottom-up strategy of photonic crystal construction is based on self assembly of colloidal particles.[13–15] Three-dimensional bulk crystals and crystalline multilayers can be prepared by natural[16,17] and controlled sedimentation,[18–21] sedimentation on a template surface,[22] solvent evaporation,[23–26] solvent depletion,[27] and assembly at vertical walls[28,29] and in confined spaces under the effect of a flow field.[30] These structures have also been prepared layer-by-layer using solvent evaporation methods.[31–34] Layer-by-layer assembly leads to altered photonic properties when the particle sizes are different in the successive layers.[35]

The Langmuir–Blodgett (LB) technique is frequently used to make monolayers of particles at the air/water or air/oil interface.[36–38] The main interest is the investigation of interaction forces between the particles[39–43] and coagulation in two dimensions.[44–48] Solid films of particles transferred from the water surface onto supports have been prepared from spread particle layers[49] and by using the technique of adsorbing nanoparticles from the aqueous subphase onto the floating charged molecular monolayers.[50,51]

Recently, one of us[52] investigated the possibility of preparing two-dimensional colloidal crystals from silica spheres by the LB method and succeeded in depositing monolayers consisting of hexagonally close-packed (hcp) arrays of silica on various substrates. The photonic properties of the silica films were observed and from the optical diffraction, the lattice parameter and the particle size were calculated, the latter in excellent agreement with data from AFM measurements. The results suggest that a successful synthesis of ordered monolayers of monodisperse silica with the LB technique critically depends on the hydrophilic/hydrophobic balance. Therefore, in the present

†Basis of a presentation given at Materials Discussion No. 5, 22–25 September 2002, Madrid, Spain.

 DOI: 10.1039/b204687c

This journal is © The Royal Society of Chemistry 2002

work, this balance was investigated by modification of the surface of the silica spheres through the adsorption of surfactants. Particle size, surface charge, and the effect of solvent were taken into account. Finally, the study was extended to multilayers. The photonic properties of the mono- and multilayers are also reported.

Experimental

Particle synthesis

Monodisperse silica particles were prepared by the method of Stöber, Fink, and Bohn[53,54] from tetraethyl orthosilicate (TEOS, BDH), ammonia (25% NH_3 solution Riedel-de Haëhn) and water (Millipore water, the resistivity was 18.2 MΩ cm, MilliQ water purification system). TEOS was added to the methanolic solution of ammonia and water in one step and the mixture was stirred for 24 h. The silica suspensions were centrifuged at 3000 rpm for 30 min and washed with water. The centrifuging/washing procedure was repeated 6 times. The particles were dried at 120 °C overnight. Three samples of different particle sizes were prepared varying the molar concentrations of TEOS, ammonia, and water, as shown in Table 1: bare silica particles with theoretical diameters of $d = 320$ (BS1) and 460 nm (BS2), and a modified silica (MS) of $d = 500$ nm. The latter was prepared by adding 0.38 mM *N*-trimethoxysilylpropyl-*N*,*N*,*N*-trimethylammonium chloride (TMSPA, Gelest, 50% methanolic solution) to the bare silica suspension in ethanol and stirring overnight. The particles were washed as described above for the bare silica samples. The modified silica was dried at 60 °C.

Particle characterization

The particle diameters were measured using SEM pictures taken with a Philips SEM 515 scanning electron microscope.

The N_2-adsorption isotherms were measured at 77 K with a Coulter Omnisorp 100 (Coulter Corporation, Hialeah, FL, USA) surface area analyzer. The specific surface area was calculated by the BET method. Prior to the measurements, the samples were heated overnight at 120 °C in a vacuum of 10^{-5} Torr.

The zeta potential of the silica samples was measured in a Zetamaster (Malvern Instruments Ltd., Worcestershire, UK) laser Doppler micro electrophoresis instrument. The particle dispersions were prepared in Millipore water, the particle concentration was 0.1 wt% and the pH approximately 6.5 for all suspensions.

The refractive index of the silica particles was determined experimentally using the index-matching method.

Preparation of monolayers and multilayers

Suspensions of bare and modified silica particles were prepared in chloroform (Fluka), methanol (Merck), or a mixture of the two. The silica concentration was 16.7 mg mL^{-1} in all experiments. The composition of the suspensions which were spread on the surface of water are collected in Table 2.

Ionic surfactants were added to the suspensions to control the hydrophilic–hydrophobic properties of the particles: cationic surfactants hexadecyltrimethylammonium bromide (C_{16}, HDTABr, Acros) and decyltrimethylammonium bromide (C_{10}, DTABr, Acros) to the BS suspensions and anionic surfactants sodium dodecylsulfate (C_{12}, SDS, Sigma) and 4-octylbenzenesulfonic acid sodium salt (C_8, OBS, Aldrich) to the MS suspensions. The surfactant concentration was set at 1.8 mM in the experiments. Additionally, the surfactant concentration was varied between 0.482 and 15.5 mM in the bare silica–DTABr–chloroform system. The effect of the medium (chloroform, methanol : chloroform or methanol) was investigated in the bare silica–DTABr system. The anionic surfactants SDS and OBS do not dissolve in chloroform. These were dissolved in ethanol and methanol, respectively, and then diluted with chloroform. The ethanol–chloroform and methanol–chloroform volume ratios were 2 : 8 and 1 : 9, respectively.

The silica suspensions were agitated in an ultrasonic bath for 30 min prior to use. The compression isotherms of the silica films at the air/water interface were measured in a Langmuir trough (Nima 611, Nima Technologies, Coventry, England). The films were compressed at a of barrier speed 20 cm^2 min^{-1}. For film deposition, we used 25 mm × 50 mm glass microscope slides cleaned in chromic acid and washed with water. The films were deposited in the upstroke direction at a speed of 1 mm min^{-1}, at pressures below the collapse pressures of the films. The latter were different for the BS and MS films. For spectrometry and SEM investigations, glass plates with films on one side only were used.

Multilayers were deposited on microscopic glass slides in the same way as described for the monolayers. The layers were allowed to dry in air at room temperature between successive depositions. We prepared a 3-layer film of bare silica sample with particles of 450 nm diameter (BS2) and four multilayer films (2, 3, 4, and 6 layers) of the modified silica sample (MS).

Characterization of the silica films

The amount of surfactant present in the silica films was measured by two methods. The concentration of DTABr was measured directly in the film by mass spectrometry with an ANCA 20-20 GSL spectrometer (Europe Scientific, Cheshire, England). The analysis was performed on the film prepared from a suspension of composition 1.8 mM DTABr–chloroform–BS2. To collect a sufficient number of particles, 5 depositions were made on 70 mm × 90 mm glass plates. The films were removed from the glass plates with a blade and used as powder, which was kept in an oven at 60 °C overnight. The carbon content was determined and the DTABr concentration was calculated from this.

The concentration of SDS was determined in the water subphase after film deposition. We adapted the Stains-all method described by Rusconi *et al.*[55] for very dilute SDS solutions. The absorption of the Stains-all (4,5,4′,5′-dibenzo-3,3′-diethyl-9-methylthiacarbocyanine bromide) cation–SDS anion complex was measured with a Lambda 12 (Perkin Elmer GmbH, Ueberlingen, Germany) UV-VIS spectrometer at $\lambda = 438$ nm. The extinction coefficient of the dye–SDS complex was 7.0×10^5 dm^3 mol^{-1} cm^{-1}. For measurements, 100 μL of 1 mg ml^{-1} Stains-all (Aldrich) solution in 50%

Table 1 Molar concentrations of reactants in the synthesis of monodisperse silica spheres of different diameters. BS: bare silica; MS: modified silica

Silica sample	*d*/nm	TEOS/M	NH_3/M	H_2O/M
BS1	320	0.25	0.9	8.0
BS2	460	0.3	1.13	6.4
MS	500	0.17	2.0	6.0

Table 2 Composition of the silica suspensions spread on the surfaceof water for LB monolayer preparation

Silica, charge	Surfactant, chain length, charge	Medium
Bare silica, negative	HDTABr, C16, positive	Chloroform
	DTABr, C10, positive	Chloroform
		Methanol–chloroform
		Methanol
Modified silica, positive	SDS, C12, negative	Ethanol–chloroform
	OBS, C8, negative	Methanol–chloroform

2-propanol–water mixture was introduced into the spectrometer cuvette and immediately diluted with 3 ml of the SDS solution taken from the subphase after the silica film deposition. Subphase samples were taken from inside and outside the dipping well and the results were averaged. The SDS concentration was determined for a film prepared by spreading the suspension of composition 1.8 mM SDS–[ethanol–chloroform (2 : 8)]–MS.

Transmission spectra of the particle monolayers and multilayers were measured in the wavelength range 300 to 2700 nm with a Cary 5 (Varian Australia Pty Ltd, Mulgrave, Australia) UV-VIS-NIR spectrometer. The incident angle dependence of the transmission spectra was measured in a sample holder with a goniometer.

Results and discussion

1 Properties of the silica particles

The properties of the spherical, monodisperse silica particles are listed in Table 3.

The average diameters measured for a large number of particles in the SEM pictures are close to the preset values given in Table 1. The polydispersity expressed as the standard deviation of the average diameter is in the range 3.8–6.9%. This is low and compares well with the polydispersity reported in the literature.[56,57]

The BET specific surface area of the particles is somewhat larger than the surface area calculated on the basis of particle geometry and an estimated particle density of 1.8 g cm^{-3}. This result agrees with earlier observations for Stöber silica particles[58,59] and is indicative of the presence of pores.

The zeta potential of the bare silica samples is *ca.* −5 mV and that of the modified silica *ca.* +30 mV. Thus, silylation with TMSP cations changes the surface charge from negative to positive. At pH 6.5, the bare silica is negatively charged, in accordance with the point of zero charge (pH 2–3).

The refractive index of the silica particles is between 1.44 and 1.45. The best particle screening was obtained in 2-methyl-1-propanol (n = 1.446). This result corresponds with the generally assumed value. Garcia-Santamaria *et al.*[60] measured the refractive index of Stöber silica particles of the same size range as our silicas. They obtained a value of 1.43 at room temperature, and up to 600 °C.

2 π–A Isotherms and monolayers

The π–A isotherms of the particle films prepared from the different surfactant–solvent–silica spreading suspensions were measured to determine the optimal surface pressure for deposition. A typical π–A isotherm is shown in Fig. 1, where the surface pressure is plotted against the area/particle mass. The shapes of the isotherms are similar for all films. Three regions can be distinguished. There is a sharp transition from the gaseous phase (region I) to the solid condensed phase

Table 3 Properties of the silica particles

	Particles		
Property	BS1	BS2	MS
Avg. particle diameter, d(SEM)/nm	357	450	550
Polydispersity, σ_d(SEM) (%)	5	6.9	3.8
BET specific surface area, S_{BET}/m^2 g^{-1}	18	11	9
Geometrical surface area,[a] S_{geom}/m^2 g^{-1}	9.3	7.4	6
Zeta potential[b]/mV	−5	−5	+30
Refractive index	1.44–1.45		

[a] $\rho_{particle}$ = 1.8 cm^3 g^{-1}. [b] Aqueous suspension, pH 6.5.

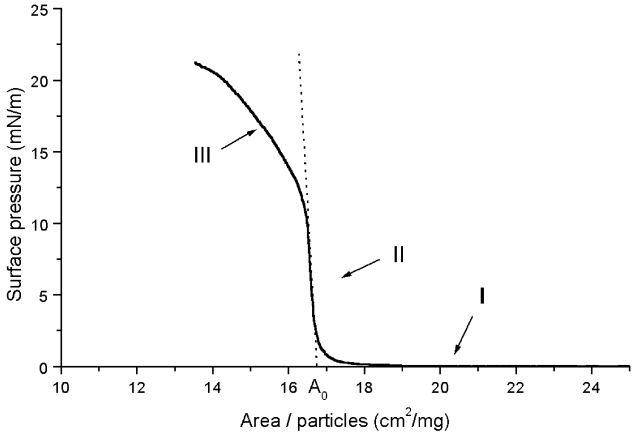

Fig. 1 π–A Isotherm of the OBS–[methanol–chloroform (1 : 9)]–MS particle film.

(region II), where the pressure increase is very steep and linear. The pressure increase is steeper than that observed for aggregated organophilic silica particle films,[45,61] indicating higher rigidity. The liquid phase region is apparently missing in the isotherms. In region III, the surface pressure increases in a non-linear fashion. We assume that the surface pressure at the transition from region II to region III is a kind of collapse pressure. This collapse pressure depends on the composition of the systems under study. The modified silica particle films collapse at about 10 mN m^{-1} (Fig. 1), and the bare silica particle films at about 5 mN m^{-1}. The particle films were deposited at pressures below these values: 5 mN m^{-1} for the modified silica and 4 mN m^{-1} for the bare silica films. The higher collapse pressure of the modified particle films (~10 mN m^{-1}) as compared to that of the bare silica particle films (~5 mN m^{-1}) could be due to the presence of a soft silylating layer on the surfaces of the modified particles. The presence of such a layer, being able to accommodate 2.8 mmol g^{-1} of chloroform, can be assumed from liquid mixture adsorption experiments, details of which will be discussed in a separate publication.[62]

The area/particle values at the onset of pressure increase (A_0 in Fig. 1) were between 16 and 17 cm^2 mg^{-1}. From the A_0 values an average particle density of 1.8 g cm^{-3} can be calculated, assuming a hexagonally close packed arrangement (the area of the hcp unit cell is $2r^2\sqrt{3}$, with r being the radius of the particles).

The amount of surfactant adsorbed on the silica spheres was measured in films deposited from suspensions with composition 1.8 mM SDS–[ethanol–chlorofom (2 : 8)]–MS and 1.8 mM DTABr–chloroform–BS2. Only one third of the added amount of SDS was adsorbed, while DTABr was quantitatively adsorbed. The adsorbed amount of SDS corresponds to 2.5 molecules nm^{-2}, half of a densely packed monolayer. The adsorbed amount of DTABr corresponds to 0.19 nm^2 per DTABr molecule. A double layer of DTABr molecules has to be assumed to accommodate all these molecules. One of the reasons for submonolayer coverage of SDS might be that SDS partially dissolves in the subphase, together with ethanol, during film formation. Thus, SDS does not fully neutralize the positive charge on the modified silica particles (zeta potential +30 mV), while DTABr overcompensates the negative charge on bare silica (zeta potential −5 mV). The resulting surface coverage in both cases is charge carrying and partially hydrophobic, which ensures dipole–dipole repulsion between the particles and moderate wetting by the subphase. The optimal combination of the two properties (surface charge and partial hydrophobicity) is necessary for ordered film formation. Uncharged hydrophobic particles tend to aggregate[61] and fully hydrophilic particles tend to escape from the interface into the

water. The latter tendency was observed in our experiments using particles without adding surfactant to the spreading suspension.

Fig. 2–4 show SEM pictures of monolayers of BS1 or BS2 modified with DTABr in chloroform (Fig. 2), a mixture of chloroform and methanol (Fig. 3), and methanol only (Fig. 4). In all cases, hcp ordering of the silica particles is observed. The domains are small and the disorder is extensive with chloroform as solvent. The size of the domains increases, however, in chloroform–methanol mixture and in methanol alone. In agreement with this observation, the number of defects (absence of silica spheres) decreases from chloroform through chloroform–methanol to methanol. Finally, in all cases, aggregates of silica particles can be seen, and these stick to the particle monolayer. The number of aggregates can be decreased by increasing the time of ultrasonic agitation of the suspensions before spreading and/or by washing the silica particles with methanol before suspension preparation.

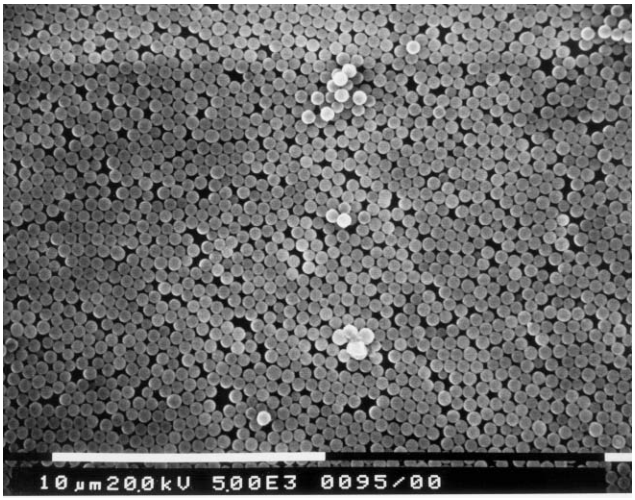

Fig. 2 SEM picture of the DTABr–chloroform–BS2 monolayer; $c_{DTABr} = 1.8$ mM, $d_{BS2} = 450$ nm.

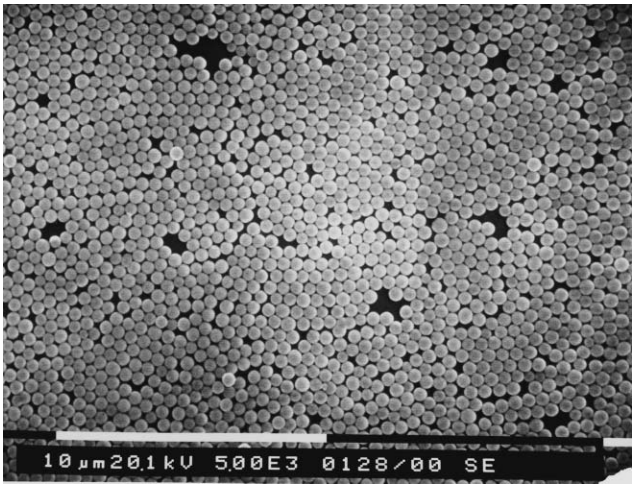

Fig. 3 SEM picture of the DTABr–[methanol–chloroform (8 : 2)]–BS2 monolayer; $c_{DTABr} = 1.8$ mM, $d_{BS2} = 450$ nm.

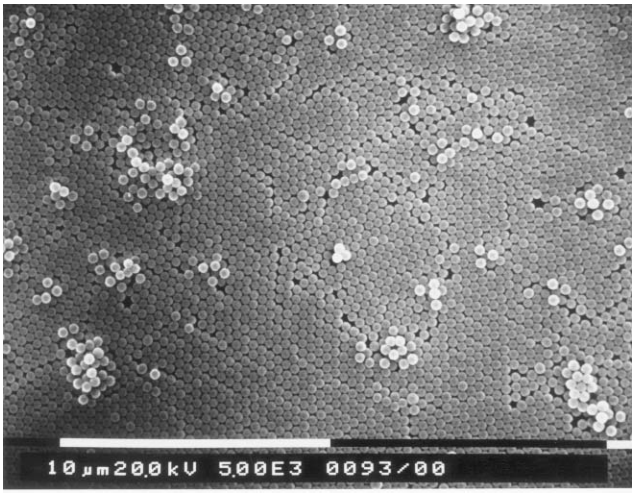

Fig. 4 SEM picture of DTABr–methanol–BS1 monolayer; $c_{DTABr} = 1.8$ mM, $d_{BS1} = 357$ nm.

There are experimental examples in the literature of loosely packed hexagonal crystalline arrays of latex or silica particles on the surface of water,[37,38,40,46] the first such ordering being demonstrated by Perrin.[63] However, hcp ordering of particles like that shown in Fig. 4 have not yet been reported for LB films. In our experiments, this is the case in methanol. The presence of small amounts of chloroform seemed to disturb long-range ordering. It is reasonable to suppose that the type of spreading solvent has a determining effect on the interaction between the silica particles. The solvent influences the wetting of the particles at the air/water interface, thus affecting the counter ion cloud formation around the particles. Hcp ordering of colloidal particles is explained by long-range attraction,[3,64–66] which appears between similarly charged particles under specific conditions in concentrated suspensions and in confined geometries. The authors of ref. 65 state that radially symmetric counter ion fluctuations can induce long-range attractions which are too weak to influence colloidal behavior.

Fig. 5 shows a SEM picture of MS–OBS film, prepared in a methanol–chloroform mixture. The hcp domains, the defects, and the aggregates of silica particles, as in the BS/DTABr film in methanol–chloroform (Fig. 4), are all clearly visible. Thus, the type of surfactant does not seem to have a significant effect on the ordering of the silica spheres.

Likewise, variation in the surfactant chain length, HDTABr (C_{16}) and DTABr (C_{10}) for the BS2 particles and SDS (C_{12}) and OBS (C_8) for the MS particles, did not change the particle ordering noticeably.

The effect of the surfactant concentration on the ordering was investigated in DTABr–chloroform–BS2 films. The DTABr concentration was varied between 0.482 and 15.1 mM. No consistent changes in the film quality due to the surfactant concentration variations were observed in this concentration range. The main characteristics of the films, the small domain size and the random crystal orientations, remained, together with defects.

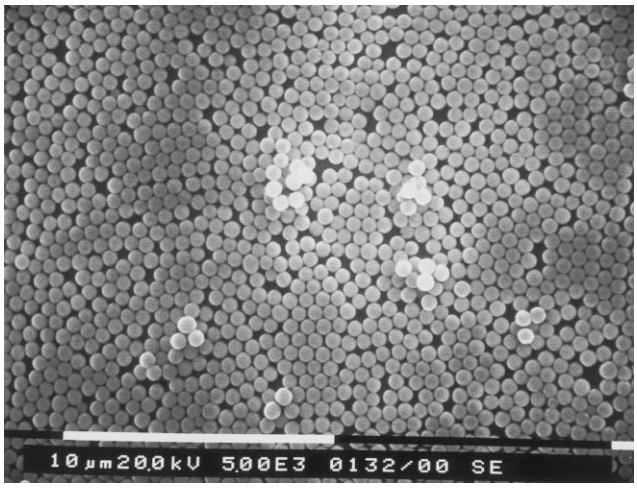

Fig. 5 SEM picture of OBS–[methanol–chloroform (1 : 9)]–MS monolayer; $c_{OBS} = 1.8$ mM, $d_{MS} = 550$ nm.

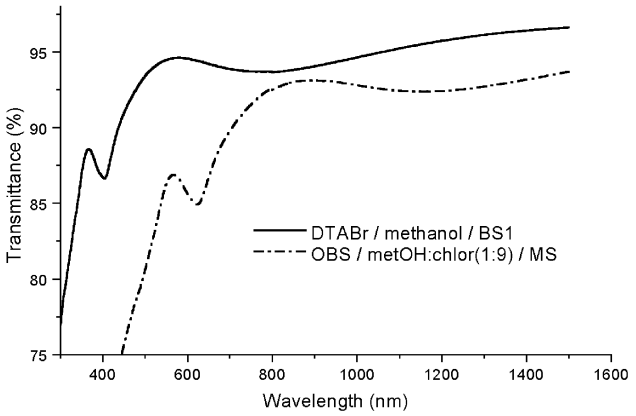

Fig. 6 Transmission spectra of monolayers prepared from suspensions of compositions indicated in the graph; $d_{BS1} = 357$ nm, $d_{MS} = 550$ nm.

Transmission spectra of silica monolayers prepared from 1.8 mM DTABr–methanol–BS1 and 1.8 mM OBS–[methanol–chloroform (1 : 9)]–MS are shown in Fig. 6. The spectra of all the monolayer films show two troughs, a broad one in the NIR region and a sharp one in the visible. These are superimposed on background scattering, which strongly depends on the type of sample. In any case, it increases strongly at shorter wavelengths. The wavelengths corresponding with the minima of the troughs for the different particle diameters are collected in Table 4. They can be ascribed to first order and second order Bragg diffractions.[16] The numbers in brackets correspond to the Bragg diffraction maxima calculated from the Bragg equation for an hcp crystal: $\lambda_{max} = 2Dn_{eff}$ for the first order and $\lambda_{max} = Dn_{eff}$ for the second order diffraction, where D is the lattice parameter ($D = 0.866d$, for an hcp crystal[67]) and n_{eff} is the effective index of refraction [$n_{eff} = f_{SiO2} \cdot n_{SiO2} + f_{air} \cdot n_{air} = (0.74 \times 1.445) + (0.26 \times 1) = 1.3293$]. For hcp packing, the volume fraction of spheres is 74%.

In the wavelength region below the second order diffraction, a strong attenuation of the transmitted light intensity is seen (Fig. 6). This is due to different factors: (1) monotonically increasing light scattering at wavelengths below the size of the particles and (2) defects in the film.[34] Overall, Fig. 6 shows that the transmission spectra of our silica monolayers resemble those of a perfect hcp monolayer of silica spheres.[34] The diffraction strength is smaller and the spectral broadening wider in our case, because of the defects in the films.

3 Multilayers

A SEM picture of the 3-layer 1.8 mM DTABr–chloroform–BS2 sample is shown in Fig. 7. The layered structure is preserved through the deposition of successive layers. When Fig. 7 is compared with Fig. 2, where a monolayer of this system composition is shown, an improvement in the ordering can be observed: the size of the hcp ordered domains increased. The defects of the monolayer can be seen also in the multilayer film. The particles in the layer are not exactly at the same height, particles at lower positions are darker, and those at higher positions lighter. There are also aggregates present, stuck to the layer on the top.

Table 4 First and second order Bragg diffractions for various particles

		Bragg diffractions[a]	
Sample	Diameter, d/nm	1st Order, λ/nm	2nd Order, λ/nm
BS1	357	820 (821)	405 (411)
BS2	450	1017 (1036)	550 (518)
MS	550	1200 (1266)	625 (633)

[a]Calculated values are given in parentheses.

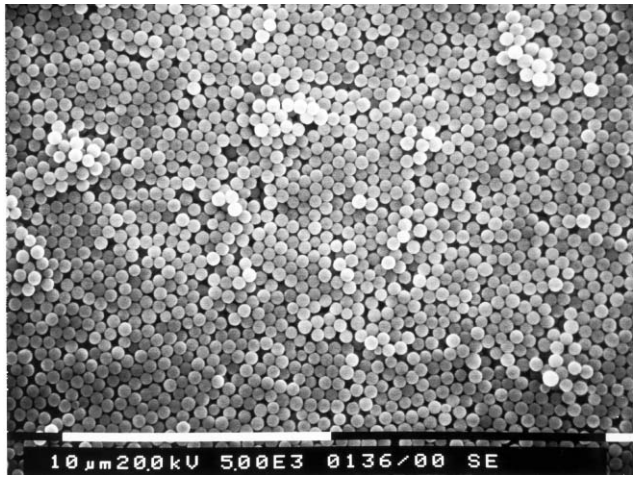

Fig. 7 SEM picture of the multilayer (3 layers) film prepared from a 1.8 mM DTABr–chloroform–BS2 suspension.

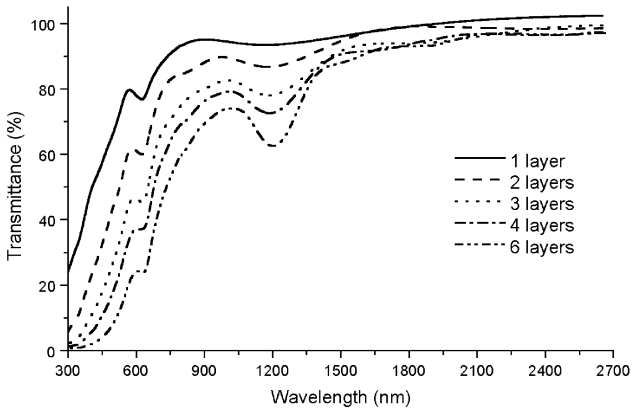

Fig. 8 Transmission spectra of the 1.8 mM OBS–[methanol–chloroform (1 : 9)]–MS multilayer films.

The transmission spectra of multilayer films prepared from a 1.8 mM OBS–[methanol–chloroform (1 : 9)]–MS suspension are shown in Fig. 8. As the layer thickness increases, the intensity of the broad attenuation peak at 1200 nm increases. At the same time, the width of the peak decreases. This behaviour is characteristic of photonic bandgap materials.[25,26] We have calculated the transmission for plane waves at normal incidence on a (111) surface using the transfer matrix method introduced by Pendry and MacKinnon[68] to calculate the propagation of the electromagnetic waves through slabs of finite thickness.[69] The theoretical transmission spectra, calculated with the experimentally determined particle size and refractive index values, give excellent agreement for the bandgap positions. With a particle diameter of 550 nm and a refractive index of 1.445 for the 6-layer 1.8mM OBS–[methanol–chloroform (1 : 9)]–MS film, the theoretical bandgap position is at 1215 nm, while the experimental value is 1200 nm. The theoretical bandgap position of the 3-layer DTABr–chloroform–BS2 film ($d = 450$ nm, $n = 1.445$) is at 1000 nm, and the experimental value is 1017 nm.

The incident angle dependence of the transmission spectra of the 6-layer 1.8 mM OBS–[methanol–chloroform (1 : 9)]–MS system is shown in Fig. 9. When the angle of light incidence with respect to the (111) plane of the multilayer crystal, θ, decreases, the first order diffraction peak at 1200 nm shifts to lower wavelengths. The transmittance decreases in the whole wavelength range, which is due to the increased background scattering (caused by the crystal defects), as the light crosses increasing widths of the sample. From the positions of the

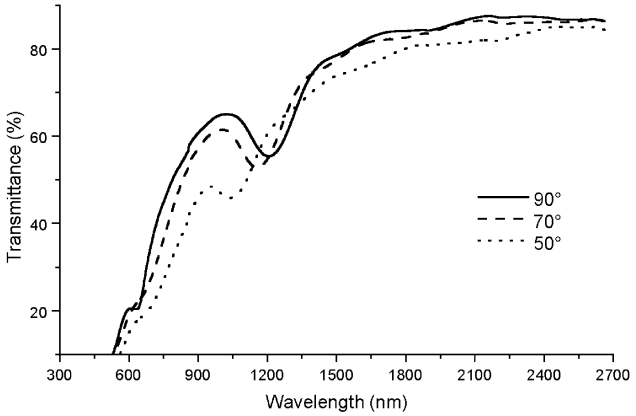

Fig. 9 Incident angle dependence of the transmission spectra of the 6-layer film prepared from the 1.8 mM OBS–chloroform–MS system. A 90° incidence angle means perpendicular to the (111) plane of the colloidal crystal.

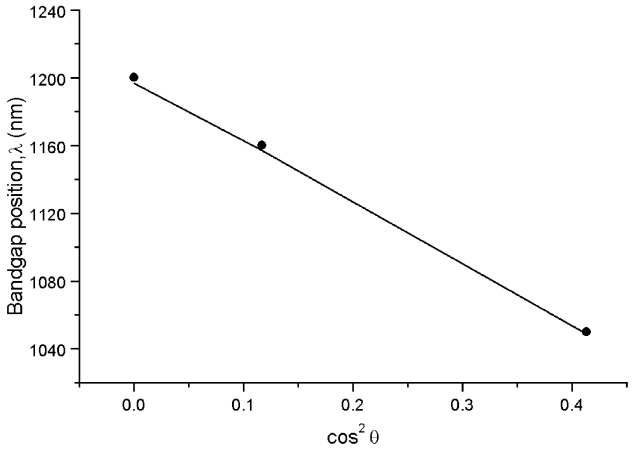

Fig. 10 Angular dispersion of the stop-band for the 6-layer 1.8 mM OBS–[methanol–chloroform (1 : 9)]–MS film. The line is a plot of the angular dispersion calculated from the Bragg equation.

bandgap at the different angles, the angular dispersion can be calculated.[70]

In Fig. 10, a plot of the bandgap positions (λ_{max}) as a function of $\cos^2\theta$ is shown for the 6-layer 1.8 mM OBS–[methanol–chloroform (1 : 9)]–MS film. This plot is a representation of the bandgap angular dispersion data in terms of the Bragg equation.[16,19] The linear dependence shows that the Bragg law applies to our silica multilayer system prepared by the LB method. The line in Fig. 10 is calculated with the Bragg equation, $\lambda_{max} = 2D\sqrt{(n_{eff}^2 - \cos^2\theta)}$, where D is the lattice parameter ($D = 0.816d$ for an fcc crystal[57]), n_{eff} is the effective index of refraction ($n_{eff} = 1.3293$, assuming 74% volume filling of the silica balls), and θ is the angle between the incident light and the (111) plane of the crystal.

Conclusions

Monolayer and multilayer films of spherical silica particles have been prepared on glass substrates using the LB method. Monodisperse silica particles prepared by the Stöber method have to be modified with surfactants prior to spreading on the water surface. All films contain hcp crystalline domains, defects and aggregates of silica particles. The largest hcp domains and the least number of defects were obtained with methanol as spreading agent. In chloroform, the hcp domains are small and the number of defects is large. Aggregates can be eliminated by washing the particles in methanol and increasing the sonication time prior to spreading.

The monolayer and multilayer silica films show photonic bandgap properties, which can be detected by transmission measurements in the visible and near infrared regions. The experimental bandgap positions are in good agreement with the theoretical positions calculated with the transfer matrix method. In the multilayer films the bandgap depth increases gradually with the number of layers. The angular dispersion of the bandgap for the 6-layer silica sample satisfies Bragg's law.

Acknowledgements

We would like to thank R. H. A. Ras for multiple discussions. This work was financially supported by the Flemish-Hungarian Bilateral Scientific and Technological Cooperation Project NR. BIL 00/10 and by the F.W.O., Flanders (contracts G. 0201.02. and G. 0261.02.). The authors are grateful to the department of Metallurgy and Materials Engineering of K.U. Leuven for providing access to the SEM instrument.

References

1 J. V. Sanders, *Acta Crystallogr., Sect. A*, 1968, **24**, 427.
2 J. B. Pendry, *Curr. Sci.*, 1999, **76**, 1311.
3 A. D. Dinsmore, J. C. Crocker and A. G. Yodh, *Curr. Opin. Colloid Interface Sci.*, 1998, **3**, 5.
4 A. J. Hurd, *J. Phys. A: Math. Gen.*, 1985, **18**, L1055.
5 J. Sun and T. Stirner, *Langmuir*, 2001, **17**, 3103.
6 O. Velev and A. M. Lenhoff, *Curr. Opin. Colloid Interface Sci.*, 2000, **5**, 56.
7 C. Liu and C. R. Martin, *Nature*, 1991, **352**, 50.
8 J. Holtz and S. A. Asher, *Nature*, 1997, **389**, 829.
9 M. J. Tierney and H. O. L.Kim, *Anal. Chem.*, 1993, **65**, 3435.
10 S. A. Asher, J. W. Holtz and G. Pan, *MRS Bull.*, 1998, **23**, 44.
11 E. Yablonovich, *Phys. Rev. Lett.*, 1987, **58**, 2059.
12 S. John, *Phys Rev. Lett.*, 1987, **58**, 2486.
13 K. Nakahama, H. Kawaguchi and K. Fujimoto, *Langmuir*, 2000, **16**, 7882.
14 D. J. Norris and Y. A. Vlasov, *Adv. Mater.*, 2001, **13**, 371.
15 V. L. Colvin, *MRS Bull.*, 2001, **26**, 637.
16 C. López, L. Vázquez, F. Meseguer, R. Mayoral and M. Ocaña, *Superlattices Microstruct.*, 1997, **22**, 399.
17 H. Míguez, F. Meseguer, C. López, A. Blanco, J. S. Moya, J. Requena, A. Mifsud and V. Fornés, *Adv. Mater.*, 1998, **10**, 480.
18 P. V. Braun, R. W. Zehner, C. A. White, M. K. Weldon, C. Kloc, S. S. Patel and P. Wiltzius, *Adv. Mater.*, 2001, **13**, 721.
19 H. Miguez, F. Meseguer, C. Lopez, M. Holgado, G. Andreasen, A. Mifsud and V. Fornes, *Langmuir*, 2000, **16**, 4405.
20 P. Jiang, J. Cizeron, J. F. Bertone and V. L. Colvin, *J. Am. Chem. Soc.*, 1999, **121**, 7957.
21 J. E. G. J. Wijnhoven and W. L. Vos, *Science*, 1998, **281**, 802.
22 G-R. Yi, J. H. Moon and S-M. Yang, *Chem. Mater.*, 2001, **13**, 2613.
23 P. Jiang, G. N. Ostijic, R. Narat, D. M. Mittelman and V. L. Colvin, *Adv. Mater.*, 2001, **13**, 389.
24 J. F. Bertone, P. Jiang, K. S. Hwang, D. M. Mittelman and V. L. Colvin, *Phys. Rev. Lett.*, 1999, **83**, 300.
25 P. Jiang, J. F. Bertone, K. S. Hwang and V. L. Colvin, *Chem. Mater.*, 1999, **11**, 2123.
26 R. Rengarajan, P. Jiang, V. Colvin and D. Mitteman, *Appl. Phys. Lett.*, 2000, **77**, 3517.
27 Y. Lu, Y. Yin, B. Gates and Y. Xia, *Langmuir*, 2000, **17**, 6344.
28 A. S. Dimitrov, *Langmuir*, 1996, **12**, 1303.
29 E. H. A. De Hoog, L. I. de Jong-van Steensel, M. M. E. Snel, J. P. J. van der Eerden and H. N. W. Lekkerkerker, *Langmuir*, 2001, **17**, 5486.
30 B. Gates, D. Quin and Y. Xia, *Adv. Mater.*, 1999, **11**, 466.
31 C. D. Duskhin, *Langmuir*, 1993, **9**, 3695.
32 D. N. Denkov, O. D. Velev, P. A. Kralchevsky, I. B. Ivanov, H. Yoshimura and K. Nagayama, *Langmuir*, 1992, **8**, 3183.
33 P. Jiang, J. F. Bertone and V. L. Colvin, *Science*, 2001, **291**, 453.
34 T. Yamasaki and T. Tsutsui, *Jpn. J. Appl. Phys.*, 1999, **38**, 5916.
35 K. P. Velikov, C. G. Christova, R. P. A. Dullens and A. van Blaaderen, *Science*, 2002, **296**, 106.
36 P. Pieranski, *Phys. Rev. Lett.*, 1980, **45**, 569.
37 C. P. Collier, R. J. Saykally, J. J. Shiang, S. E. Henrich and J. R. Heath, *Science*, 1997, **277**, 1978.

38 D. G. Kurth, P. Lechmann and C. Lesser, *Chem. Commun.*, 2000, 949.
39 A. J. Armstrong, R. C. Mockler and W. J. O'Sullivan, *J. Phys. Condens. Matter*, 1989, **1**, 1707.
40 D. J. Robinson and J. C. Earnshaw, *Langmuir*, 1993, **9**, 1436.
41 R. Aveyard, B. P. Binks, J. H. Clint, P. D. I. Fletcher, B. Neumann, V. N. Paunov, J. Annesley, D. Nees, A. W. Parker, A. D. Ward and A. N. Burgess, *Central Laser Facility Annual Report 2000/2001*, CLRC Rutherford Appleton Laboratory, Didcot, Oxfordshire, UK, 2001.
42 J. Sun and T. Stirner, *Langmuir*, 2001, **17**, 3103.
43 F. Martínez-López, M. A. Cabrerizo-Vílchez and R. Hidalgo-Álvarez, *J. Colloid Interface Sci.*, 2000, **232**, 303.
44 Gy. Tolnai, F. Csempesz, M. Kabai-Faix, E. Kálmán, Zs. Keresztes, A. L. Kovács, J. J. Ramsden and Z. Hórvölgyi, *Langmuir*, 2001, **17**, 2683.
45 F. Ghezzi, J. C. Earnshaw, M. Finnis and M. McCluney, *J. Colloid Interface Sci.*, 2001, **238**, 433.
46 D. J. Robinson and J. C. Earnshaw, *Phys. Rev. A*, 1992, **46**, 2045; D. J. Robinson and J. C. Earnshaw, *Phys. Rev. A*, 1992, **46**, 2055; D. J. Robinson and J. C. Earnshaw, *Phys. Rev. A*, 1992, **46**, 2065.
47 A. J. Hurd and D. W. Schaeffer, *Phys. Rev. Lett.*, 1985, **54**, 1043.
48 G. Y. Onoda, *Phys. Rev. Lett.*, 1985, **55**, 226.
49 L. Cao, H. Wan, L. Huo and S. Xi, *J. Colloid Interface Sci.*, 2001, **244**, 97.
50 K. Muramatsu, M. Takahashi, K. Tajima and K. Kobayashi, *J. Colloid Interface Sci.*, 2001, **242**, 127.
51 S. A. Iakovenko, A. S. Trifonov, A. Mamedov, D. K. Nagesha, V. V. Hanin, E. C. Soldatov and N. A. Kotov, *Adv. Mater.*, 1999, **11**, 388.
52 B. van Duffel, R. H. A. Ras, F. C. De Schryver and R. A. Schoonheydt, *J. Mater. Chem.*, 2001, **11**, 3333.
53 W. Stöber, A. Fink and E. Bohn, *J. Colloid Interface Sci.*, 1968, **26**, 62.
54 P. W. Hsu, R. Yu and E. Matijević, *J. Colloid Interface Sci.*, 1993, **156**, 56.
55 F. Rusconi, É. Valton, R. Nguyen and E. Dufourick, *Anal. Biochem.*, 2001, **295**, 31.
56 D. Peng, *Prog. Nat. Sci.*, 1999, **10**, 575.
57 R. Mayoral, J. Requena, J. S. Moya, C. López, A. Cintas, H. Míguez, F. Meseguer, L. Vázquez, M. Holdago and Á. Blanco, *Adv. Mater.*, 1997, **9**, 257.
58 M. Szekeres, I. Dékány and A. de Keizer, *Colloids Surf., A.*, 1998, **141**, 327.
59 M. Szekeres, J. Tóth and I. Dékány, *Langmuir*, 2002, **18**, 2678.
60 F. Garcia-Santamaria, E. Palacios, H. Migues, M. Ibisate, F. Meseguer and C. López, *Langmuir*, 2002, **18**, 1942.
61 Z. Hórvölgyi, S. Németh and H. J. Fendler, *Langmuir*, 1996, **12**, 997.
62 I. Dékány, M. Szekeres and R. Schoonheydt, *Surface Characterization of Stöber Silica by Liquid Mixture Adsorption*, manuscript in preparation.
63 J. Perrin, *Ann. Chim. Phys*, 1909, **18**, 1.
64 D. G. Grier, *J. Phys.: Condens. Matter*, 2000, **12**, A85.
65 A. Gopinathan, T. Zhou, S. N. Coppersmith, L. P. Kadanoff and D. G. Grier, *Europhys. Lett.*, 2002, **57**, 451.
66 J. C. Crocker and D. G. Grier, *Phys Rev. Lett.*, 1996, **77**, 1897.
67 J. M. Schultz, *Diffraction for Materials Scientists*, Prentice-Hall, Englewood Cliffs, NJ, 1982.
68 J. B. Pendry and A. MacKinnon, *Phys. Rev. Lett.*, 1992, **69**, 2772.
69 A. Reynolds, F. Lopez-Tejeira, D. Cassagne, F. J. Garcia-Vidal, C. Jouanin and J. Sanchez-Dehesa, *Phys. Rev. B*, 1999, **60**, 11422.
70 S. G. Romanov, A. V. Fokin and R. M. De La Rue, *J. Phys.: Condens. Matter*, 1999, **11**, 3593.